Article

Symmetry of the Human Head—Are Symmetrical Models More Applicable in Numerical Analysis?

Monika Ratajczak [1], Mariusz Ptak [2,*], Artur Kwiatkowski [3], Konrad Kubicki [4], Fábio A. O. Fernandes [5], Johannes Wilhelm [6], Mateusz Dymek [2], Marek Sawicki [2] and Sławomir Żółkiewski [7]

[1] Faculty of Mechanical Engineering, University of Zielona Gora, Szafrana 4, 65-516 Zielona Gora, Poland; m.ratajczak@iimb.uz.zgora.pl

[2] Faculty of Mechanical Engineering, Wroclaw University of Science and Technology, Lukasiewicza 7/9, 50-371 Wroclaw, Poland; mateusz.dymek@pwr.edu.pl (M.D.); sawicki.marek@pwr.edu.pl (M.S.)

[3] Department of Neurosurgery, Provincial Specialist Hospital in Legnica, Iwaszkiewicza 5, 59-220 Legnica, Poland; artur.kwiatkowski@szpital.legnica.pl

[4] Department of Neurosurgery, Wroclaw Medical University, Ludwika Pasteura 1, 50-367 Wroclaw, Poland; konrad.kubicki@umed.wroc.pl

[5] TEMA—Centre for Mechanical Technology and Automation, Department of Mechanical Engineering, Campus de Santiago, University of Aveiro, 3810-193 Aveiro, Portugal; fabiofernandes@ua.pt

[6] CFturbo GmbH, Unterer Kreuzweg 1, 01097 Dresden, Germany; johannes.wilhelm@cfturbo.com

[7] Faculty of Mechanical Engineering, Silesian University of Technology, Konarskiego 18a, 44-100 Gliwice, Poland; slawomir.zolkiewski@polsl.pl

* Correspondence: mariusz.ptak@pwr.edu.pl; Tel.: +48-713-202-946

Abstract: The study of symmetrical and non-symmetrical effects in physics, mathematics, mechanics, medicine, and numerical methods is a current topic due to the complexity of the experiments, calculations, and virtual simulations. However, there is a limited number of research publications in computational biomechanics focusing on the symmetry of numerical head models. The majority of the models in the researched literature are symmetrical. Thus, we stated a hypothesis wherever the symmetrical models might be more applicable in numerical analysis. We carried out in-depth studies about head symmetry through clinical data, medical images, materials models, and computer analysis. We concluded that the mapping of the entire geometry of the skull and brain is essential due to the significant differences that affect the results of numerical analyses and the possibility of misinterpretation of the tissue deformation under mechanical load results.

Keywords: finite element head model; symmetry; head biomechanics; brain; skull; human asymmetry

1. Introduction

In the surrounding world, symmetry manifests itself in various forms: in painting, sculpture, architecture, music, and above all, it occurs in nature. Bearing in mind all the goods of humanity, it should be noted that people have aesthetic preferences for symmetry ranging from culture and purchasing choices to partner selection. Symmetry issues are significant in physics. There are many examples on this topic. One of them may be the symmetry of the molecules; it depends on symmetry as to whether it has a dipole moment. This has a significant impact on the electric permeability of the substance composed by these molecules.

Moreover, the symmetry of molecules in aqueous solutions of organic substances depends on whether they twist the plane of polarisation of the light passing through the medium or not. On the other hand, the symmetry of a crystal with ionic or polarised bonds determines whether it has piezoelectric properties. Of course, the issues of symmetry constantly arise in the education process. For example, in mechanics, when discussing the moment of inertia of rigid bodies; in electromagnetism, when considering the fields of charge systems; and in optics, when discussing diffraction on holes or the phenomenon

of birefringence and in elements of quantum mechanics. Thus, literature studies show that symmetry sensitivity is the subject of research by many scientists in various fields of science, ranging from psychology to neurobiology and mathematics to physics.

1.1. Facial Symmetry

Studies have shown that adults detect symmetrical images faster and more accurately than asymmetric images and remember them better [1,2]. In addition, people find more symmetrical faces to be more attractive, have a better immune system, and are more resistant to upper respiratory tract infections (Figure 1). Sasaki et al., using functional imaging, showed that symmetrical visual patterns induce greater activation in the pattern cortex [3]. In contrast, research by Makin et al. [4] using electroencephalograph (EEG) showed a more significant, sustained posterior negative potential when viewing symmetric patterns in entrainment with random [4]. Facial symmetry is considered a measure of developmental stability (also prenatal) and may indicate the so-called hereditary genetic quality, which in biological sciences, is broadly understood as the organism's chances of passing on its genes to the next generations [5].

Figure 1. Manipulation with facial symmetry: (**a**) upper row: original faces; (**b**) lower row: symmetrical faces [6].

The striking external symmetry of the skull, in contrast to its asymmetrical inner pneumatised spaces, is another proof of the importance of symmetry as a physiological health indicator for behavioural mating choices [7]. Nevertheless, it should be emphasised that the symmetry problem of the head's structures plays an essential role in disciplines such as anthropology and clinical anatomy and by proxy also an important role in clinical disciplines, such as neurosurgery, craniofacial surgery, and reconstructive surgery. While those last two will benefit immensely from studying bone symmetry, in neurosurgery, the main focus is the symmetry of cortical structures, both in anatomical and functional meaning, with an important exception in the field of pediatric neurosurgery and treatment of craniosynostoses.

1.2. Skull Symmetry

In general, modern human skulls present minor asymmetry with a dominance of the left side of the neurocranium and almost absence of asymmetry in the facial part of the skull [8]. In the modern Greek population, the left side of the skull tends to be more pronounced [9]. In this study of the modern Greek population by Chovalopoulou et al. [9], no significant directional asymmetry differences between the sexes were found. Intrapopulational index of skull asymmetry, known as fluctuating asymmetry (FA), can be interpreted as a marker of populational health and developmental stability [8]. Myslobodsky et al. [10] suggested that this calvarial asymmetry can be found as early as in infancy and be attributed to deformities linked to head turning in supine position, which correlates with handedness. In this study, mixed-handed children tended to have a flattened skull in

the right occipital area [10]. The inside of the skull also tends to present some degree of asymmetry. One example is the paranasal sinuses that are rarely symmetrical, usually separated by septum, and usually located slightly off the midline (Figure 2a). Another of the many examples of asymmetry may be the nasal cavity, the septum of the sphenoid sinus, or mastoid cells Figure 2b).
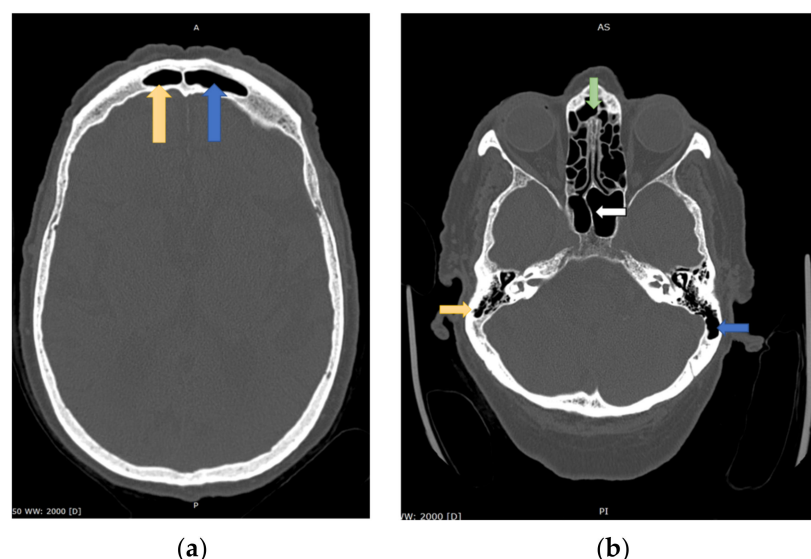

(a)   (b)

Figure 2. (**a**) Example of asymmetry of the frontal sinuses. Left one (blue arrow) is larger than right (yellow arrow); (**b**) Example of asymmetry of the: the nasal cavity (green arrow), the septum of a sphenoid sinus, mastoid cells, and the inner ear on the left (blue arrow) and the right (yellow arrow) (own source).

According to Zilles et. al. [11], the impressions on the inside of the cranial vault bones differ in their depth between two sides of the body and represent a degree of asymmetry matching the asymmetry of the brain petalia [11]. Moreover, we can point to high variability in the skull-base foramina size, with the biggest differences between diameters of the left and the right carotid canal and foramen ovale. [12]. In the Greek population examined by Chovalopaulou et al., the highest FA was found in the skull-base region [9]. The clinical importance of asymmetry of jugular foramen was suggested by Distriquin et al. in their paper in which they indicated a direct relation between the posttraumatic asymmetry of skull-base foramina and symptoms of the post-concussion syndrome [13].

1.3. Brain Symmetry

In neurosurgery, an issue of hemispheric dominance, which is closely related to brain symmetry, is a major area of interest in neuro-oncology and epilepsy surgery. It is also an essential part of vascular neurology and epileptology. Studying morphological and functional asymmetries between two hemispheres can deliver some important information about the symptomatology of the disease. Kong et al. [14] showed in their research the magnitude of the interhemispheric difference effect for both the thickness and surface area of the cerebral cortex (Figure 3) [14]. Nevertheless, cerebrum asymmetries or even neuraxis as a whole is not restricted to humans but is widespread in all vertebrates and can be found even in invertebrates [15].

During one's lifetime, a change of a hemispheres asymmetry degree can be found in radiological studies. According to Geschwind and Levitsky [16], in the general population, the left temporal planum tends to be more pronounced. However, most children of one to three years old tend to have a more developed right temporal lobe [17]. Similarly, a study of infant cadavers done by Chi et al. [18] proved that the right hemisphere's complexity is greater during infancy. Therefore, some data suggest that during the growth and maturing of the central nervous system, asymmetry of the temporal regions shifts from right-side

dominance to left-side dominance [18]. Cortical thickness shows leftward asymmetry, which is even more pronounced in males. On the other hand, different cerebrum regions are more developed in females [19]. Asymmetry can also be seen in the precentral gyrus, middle frontal, anterior temporal gyrus, and superior parietal lobule, which tends to be more prominent on the left side. In contrast, the inferior posterior temporal lobe and inferior frontal lobe of the right hemisphere are usually bigger [19]. Some environmental factors play a role in shaping the asymmetry of the hemispheres. For example, the temporal plane and precentral cortex are found to be bigger on the dominant side in trained musicians [20,21]. In a paper by Maguire et al. [22], posterior parts of hippocampi were more extensive in the London taxi drivers' population. This difference was even more pronounced on the right side.
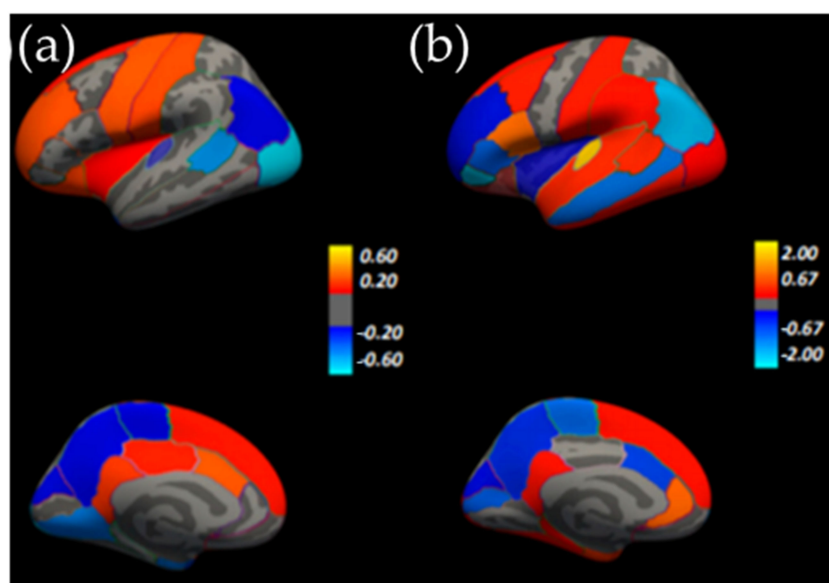

Figure 3. Brain asymmetry (**a**) in cortical thickness; (**b**) in surface area. Positive asymmetry (**a**), left side; red in (**b**) indicates leftward asymmetry, while negative asymmetry (**a**), right side; blue in (**b**) indicates rightward asymmetry (own modification based on Kong et al.) [14].

In the latter years of life, asymmetry of the hemisphere diminished and was described with measurements of the thickness of the cortex of high-order regions of the brain by Roe et al. [23]. In this study, it was proven that cortex-thickness asymmetry was smaller in elderly patients in comparison with magnetic resonance imaging (MRI) examinations from young adulthood. These changes were even more evident in patients with Alzheimer's disease. These studies suggest that during one's lifetime, there will be a variability in brain asymmetry. Most probably, the complexity and sturdiness of hemispheres will shift from right to left and, in some cases, may be affected by lifestyle and occupation. Then eventually, asymmetry of hemispheres will be lost to a degree with the ageing of the CNS. It should be emphasised here that, in general, the shrinking of the grey and white tissue is generally symmetrical. Still, some vascular changes that accumulate with age despite no neurological signs or symptoms might be more prominent on one side of the brain (Figure 4).

1.4. Numerical Head Model Symmetry

Numerical models of the human body, which are developed based on medical images, as one of the few research methods, currently provide insight into the global and local tissue response under mechanical loading [24–27]. It should be noted that this type of numerical analysis allows at a later stage to design elements that support human life functions and protect life by improving security systems [28–30]. Several numerical models of the human body have been developed that emphasise the essence of symmetry in numerical

analyses [31,32]. However, due to the difficulty of modelling soft tissues, special attention should be paid to the nervous tissue. The current literature review shows that most of the numerical models of human heads have been developed symmetrically. The following Table 1 represents a comparison of numerous adult and child brain models available for numerical studies. As visible, geometric symmetry is applied in 16 out of 22 models with respect to the sagittal plane. Two child numerical models are not reported. There are 3 available non-symmetrical adult head models and one child head model. The applicability of symmetrical head models is tempting when it comes to computational time analysis. However, the geometry resemblance is very poor. Human brain geometry is composed of the sulcus, which are grooves in the grey matter. The main advantage of non-symmetrical head models is the accuracy of brain behaviour and deformation mapping during the impact. It was noticed by Ghajari et al. [33] that the developed brain model will allow a detailed investigation of brain deformation during impact loading, especially the differences between sulci and gyri deformation. There is a tendency to create models with the highest accuracy and lowest computational time. Unfortunately, these two aspects do not go in pair. Hopefully, with the computer units development, it will be possible to calculate the most complicated models within hours.
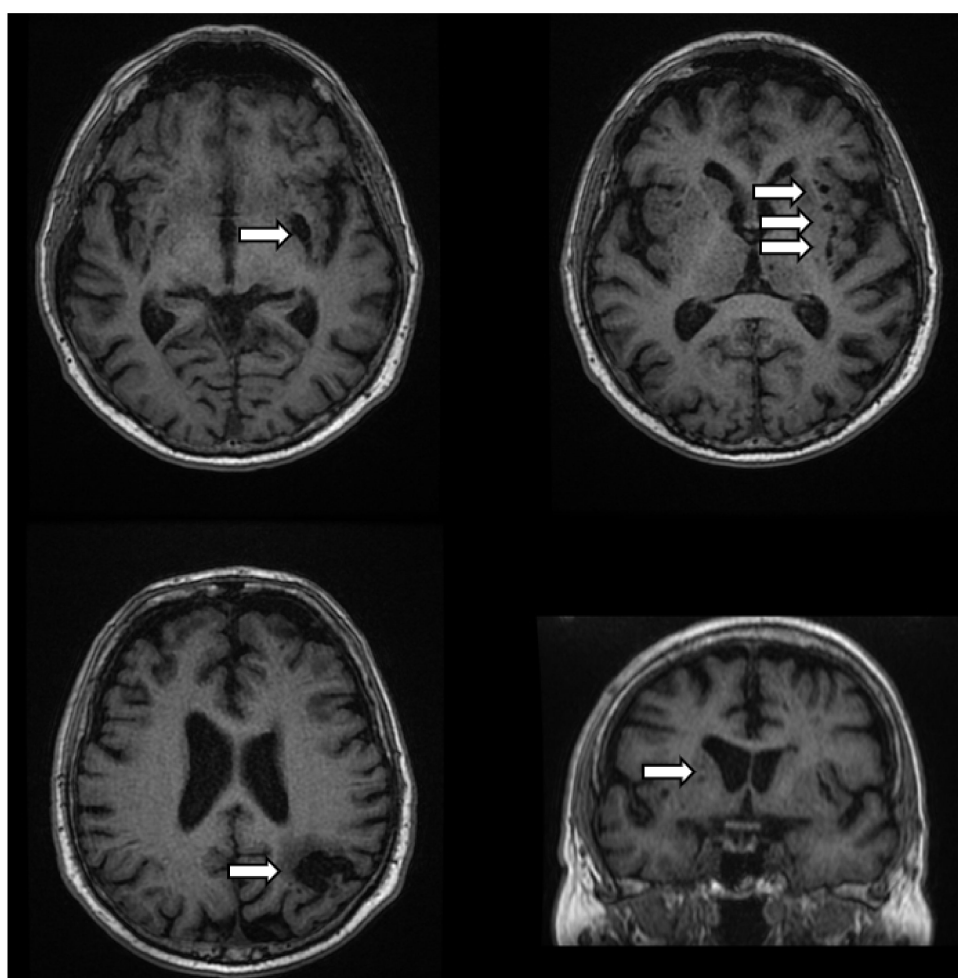

Figure 4. MRI scans of the 67-year-old patient with no neurological abnormalities but evident asymmetric lacunes (arrows), which were found coincidentally.

Table 1. Numerical head models.

Author(s)	Model Description	Geometrical Symmetry
Adult head model		
Zhang et al. [34]	Head geometry of a 50-centile adult man; anatomical drawings. Mass: 4.5 kg; number of elements: 314,500 Linear viscoelastic brain material, elasto-plastic skull material, elastic material for dura matter and skin.	Yes
Zhang et al. [35]	Model I and II. Number of elements: 4501 Anatomical drawings. Mass: 4.107 kg. Linear viscoelastic brain material, elastic behaviour for cerebrovascular elements.	Yes
King et al. [36]	The newest WSUBIM model, including viscoelastic brain and elastic-plastic skull behaviour, number of elements: 314,500.	Yes
Kleiven and Hardy [37]	Finite Element Head Model (KTH FEHM) developed in Kungliga Tekniska Högskolan (Royal Institute of Technology), number of elements: 18,400 Model consisting of skin, skull, cerebrovascular, cerebrospinal fluid (CSF), 11 bridging vein pairs, and simplified neck. Sliding connection between skull and brain.	Yes
Kleiven [38]	11,454 hexahedral elements, 6940 four-node elements, 22 two-node elements truss type Hyperelastic and viscoelastic materials for brain tissue, linear-elastic for skull, skin, and dura matter.	Yes
Horgan and Gilchrist [39]	University College Dublin Brain Trauma Model (UCDBTM) model. Consisting of: three-layered skull, dura matter, cerebrospinal fluid, falx, tentorium, separate hemispheres, cerebellum, and brain stem. Linear viscoelastic brain material, elastic material for skull and skin, mixed elements for cerebrospinal fluid.	Yes
Takhounts and Eppinger [40]	Number of elements: 45,875; brain model consisting of: skull, dura matter, cerebrospinal fluid based on outer brain layers, and brain.	Yes
Zong et al. [41]	Simplified model consisting of three-layered non-uniform skull, incompressible cerebrospinal fluid, and homogenous brain.	Yes
Belingardi et al. [42]	Numerical model generated from CT scans of 31 year old patient, composed of scalp, 3-layered-skluu, facial bones, dura matter, CSF, brain tissues, ventricles, falx, and tentorium membrane	Yes
Xiaogai Li et al. [43]	Detailed and Personalizable Head Model with Axons for Injury Prediction (ADAPT) is based on ICBM152 template generated from 152 healthy subjects. The head model includes the brain, skull (compact and diploe porous bone), meninges (pia, dura, falx, and tentorium), CSF, and superior sagittal sinus. Hyper-viscoelastic material is prescribed for brain structure.	Yes
Mao et al. [44]	Global Human Body Consortium (GHBMC) is based on MRI scans collected from an average adult male. The model consists of facial tissue, scalp, and separate brain structures, such as cerebrum gray, cerebellum, thalamus, brainstem, basal ganglia, CSF, 3rd ventricle, later ventricle, corpus callosum, cerebrum white dura, falx, and pia	Yes
Sahoo et al. [45]	Strasbourg University Finite Element Head Model (SUFEHM) is composed of scalp, brain, brainstem, cerebrospinal fluid (CSF), skull, face, and two membranes (the falx and the tentorium).	Yes
Atsumi et al. [46]	The Fe head model is an advanced model from the head model of THUMS Ver. 3. The brain consists of separate parts, such as cerebrum, cerebellum, stem, dura, arachnoid, pia, falx, CSF, and superior sagittal sinus. The mesh size and fineness are almost the same as THUMS Ver. 3; contact conditions and material properties are updated to improve computational stability and accuracy to physical model.	Yes

Table 1. *Cont.*

Author(s)	Model Description	Geometrical Symmetry
Adult head model		
Fernandes et al. 2018 [47]	Yet Another Head Model (YEAHM) consists of skull, CSF, and brain. The brain model has all important sections: frontal, parietal, temporal and occipital lobes, cerebrum, cerebellum, corpus callosum, thalamus, midbrain, and brain stem. Nonlinear, viscoelastic model for brain material, hyperelastic model for cerebrospinal fluid, and isotropic linear elastic material for skull material.	No
Ratajczak et al. 2019 [48]	αHEAD brain model consisting of skull, dura matter, falx cerebri, tentorium cerebelli, sinus sagittalis superior, bridging veins, hemispheres, and cerebellum. Number of elements: solid—55,117, shell—3784, beam—133	No
Ghajari et al. 2016 [33]	Imperial College London head model based on a 34-year-old male subject, consisting of skin, skull, cerebrospinal fluid, and brain. Falx, tentorium, and pia matter were modelled as shell elements.	No
Ji et al. 2015 [49]	Worcester head injury model (WHIM) consists of the scalp, skull, cerebrum, cerebellum, brain stem, corpus callosum, cerebrospinal fluid, ventricles, sinus, falx cerebri, tentorium cerebelli, pia mater, dura mater, facial bone, mandible, facial muscle, masseter, temporalis, submandibular soft tissue, detailed ocular structures, and teeth. The total mass is 3.569 kg.	Yes
Child head model		
Wilhelm et al. (aHEAD project 2020) [50]	aHEAD child model—2-year-old child head model. The model consists of: separate hemispheres with white and gray matter, cerebellum, brainstem, pia matter, dura matter, superior sagittal sinus, transversal sinus, bridging veins, cerebrospinal fluid, corpus callosum, and skull divided to lamina interna and externa. The validation process distinguished hyperelastic and viscoelastic material differences.	No
(DeSantis) Klinich [51]	Six-month-old child head model, viscoelastic brain material, elastic skull, and skin	No data
Roth et al. [52]	Six-month-old child head model, viscoelastic brain material, elastic skull material, cerebrospinal fluid, and skin. Number of elements: solid—69,324, shell—9187	Yes
Roth et al. [53]	Three-year-old child head model, viscoelastic brain material, elastic skull material, cerebrospinal fluid, and skin. Number of elements: solid—23,000, shell—3500	Yes
Coats et al. [54]	One-and-a-half-month-old child head model, Ogden brain material characteristics, elastic skull, and skin	No data

1.5. Validation of Numerical Models Symmetry

Finite element head models have been used to understand and predict the head response under several impact conditions. These models allow an accurate computational-based prediction of brain injuries by relating the results to medical investigations based on autopsies of corpses involved in real accidents [28]. Over the decades, a few studies were made on human cadavers. Experiments such as the ones described in Nahum et al. [29] and Hardy et al. [30] are usually used to assess intracranial pressure response and brain motion, respectively, being simulated as benchmark tests in the validation of finite element head models.

The experiments from Hardy et al. [55] are usually simulated to validate the motion of the brain model. One of these experiments is the C755-T2, being one of the most employed to validate finite element head models [48,56]. This particular one corresponds to an occipital impact with a velocity of 2 m/s. The local brain motion was measured by tracking neutral-density targets (NDTs) in these experiments, using a high-speed bi-

planar X-ray system during different impact conditions. The NDTs were implanted in two vertical columns, posterior, and anterior columns located at the occipito-parietal and the temporo-parietal regions, respectively. In the coronal plane, the two columns were approximately aligned with the right eye. The brain model nearest nodes to the position of NDTs are usually chosen to analyse the brain motion during the simulation, comparing the displacement-time history for NDTs (x-direction and z-direction) at the temporo-parietal and the occipito-parietal regions. However, both NDTs columns were inserted in the right hemisphere, as in other experiments found in Hardy's works.

As previously referred, the validation of the models is a necessary step in their development to guarantee that the computed results match the experimental data. In the literature, some experiments are considered the benchmark, for instance, the cadaveric intracranial and ventricular pressure data of Nahum et al. [57] and relative brain/skull displacement data of Hardy et al. [55,58]. The brain asymmetry and non-symmetrical modelling of finite element head models gain even more significance by analysing in detail the experiments used to validate these models. The experiments from Hardy et al. [55,58] have been used for validation of the brain motion, the brain displacement relative to the skull. However, the data were measured mainly on the same hemisphere. There are only two cases where NDTs were placed in both hemispheres: cases C380 and C393 [58]. Nevertheless, in these two, the impact direction is aligned with the NDTs plane, not being possible to verify experimentally the mirroring between NDTs displacement based on a symmetry plane between both hemispheres and mirrored NDTs coordinates.

Due to the large number of symmetrical numerical models and emphasising the asymmetry of healthy brains in the clinical literature, the authors of the study undertook research on the symmetry of the cerebral hemispheres on the developed numerical models of an elderly person and the head of a young child.

2. Materials and Methods

2.1. Development of Numerical Models of the Head of a Young Child and the Elderly

A numerical model of the head of a 2-year-old child [50] and a 77-year-old person was developed. In this concern, it was necessary to gather data of a patient without pathology in the form of DICOMs. Medical images were obtained from Provincial Specialist Hospital in Legnica, Lower Silesia Specialist Hospital of T. Marciniak and University Hospital of Wroclaw, Poland. According to the initial craniometrical catalogue, one data set for establishing the envisaged Finite Element Head Model was chosen. The work on generating models and geometric data was carried out by working directly on DICOM datasets. Dedicated open-source 3D Slicer software allows loading and connecting several different medical imaging sets simultaneously. The head model of a child and an elderly person was fully manually segmented. The left and right hemispheres of the brain were distinguished. The threshold filters in the program allow application only to the preselection of a complex of parts. This circumstance forces to clear the preselection manually; it is a gradual work that has to be done picture by picture. Greater effort reveals the overall external geometry of the brain, including the refined structure of bends and furrows at a more convenient level of detail. The data's proceeding resulted in an accurate geometrical (CAD) model, which was translated into a discrete (CAE) model for proceedings within the LS-DYNA code. The main aspect has to be seen in the envisaged calculability of the model in a timely manner by ensuring a high level of detail in both model and results. Material data for individual head structures were determined based on the literature [48,50,59,60].

2.2. The Method of Checking the Symmetry in Numerical Models of the Human Head

The two brain hemispheres of the numerical head model in a 2-year-old child and a person aged 77 were compared. The analysis considered the mass of white and grey matter, the total number of finite elements, and the cerebral hemisphere's total mass. In addition, based on the obtained geometry from the DICOMs, we carried out deviation analysis, i.e., the quantitate comparison between surface distances. In the deviation analysis, the right

part of the brain is mirrored according to the plain crossing the brain's CoG and compared to the left part, i.e., the left hemisphere is the reference.

3. Results

The difference between the total number of finite elements and the mass between the left and right hemispheres are presented in Table 2. The differences between the structures (right/left) are ~1% for both the 2-year-old and 77-year-old head models.

Table 2. The compartment of brain structures' mass and the number of finite elements used to model 2-year-old and 77-year-old heads. The FE models are depicted for the structures.
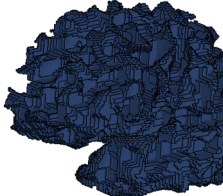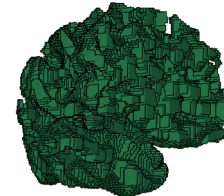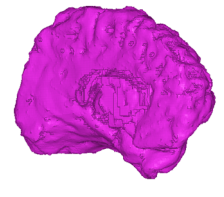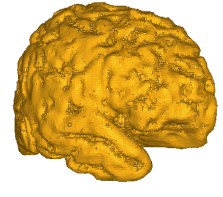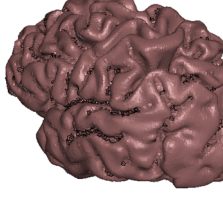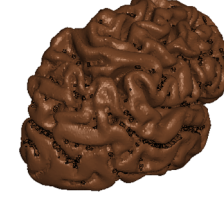
Brain Structure No. of FEs and Mass	Child: 2 Year Old—Hemisphere:		Senior: 77 Year Old—Hemisphere:	
	Left	**Right**	**Left**	**Right**
White Matter	233,760 0.242781 kg	245,830 0.255368 kg	231,146 0.238867 kg	237,494 0.245465 kg
Grey matter	208,498 0.135695 kg	201,127 0.130257 kg	313,176 0.189834 kg	311,954 0.187494 kg
Total #FEs	442,258	446,957	544,322	549,448
Total mass	0.378476 kg	0.385625 kg	0.428701 kg	0.432959 kg

Figure 5 depicts the distribution of hexahedral finite element volumes for the skull and the brain for both the 2-year-old and 77-year-old head models. We can observe the non-symmetry of the FE distribution caused by at least two factors: the asymmetry of the head geometry and, for the skull, the asymmetrical distribution of the skull thickness across the model.

Basing on the obtained geometry from the DICOMs, we carried out deviation analysis, i.e., the quantitate comparison between surface distances (Figure 6). In the deviation analysis, the right part of the brain is mirrored according to the plain crossing the brain's CoG and compared to the left part, i.e., the left hemisphere is the reference. The analysis enabled the authors to present the asymmetry of sulci and gyri for the hemispheres. We can observe a bigger deviation for the 77-year-old brain model (~10.9 mm for 14.69% of the surface), whereas for the child's model, the deviation is smaller (~7.6 mm for 12.03% of the surface).
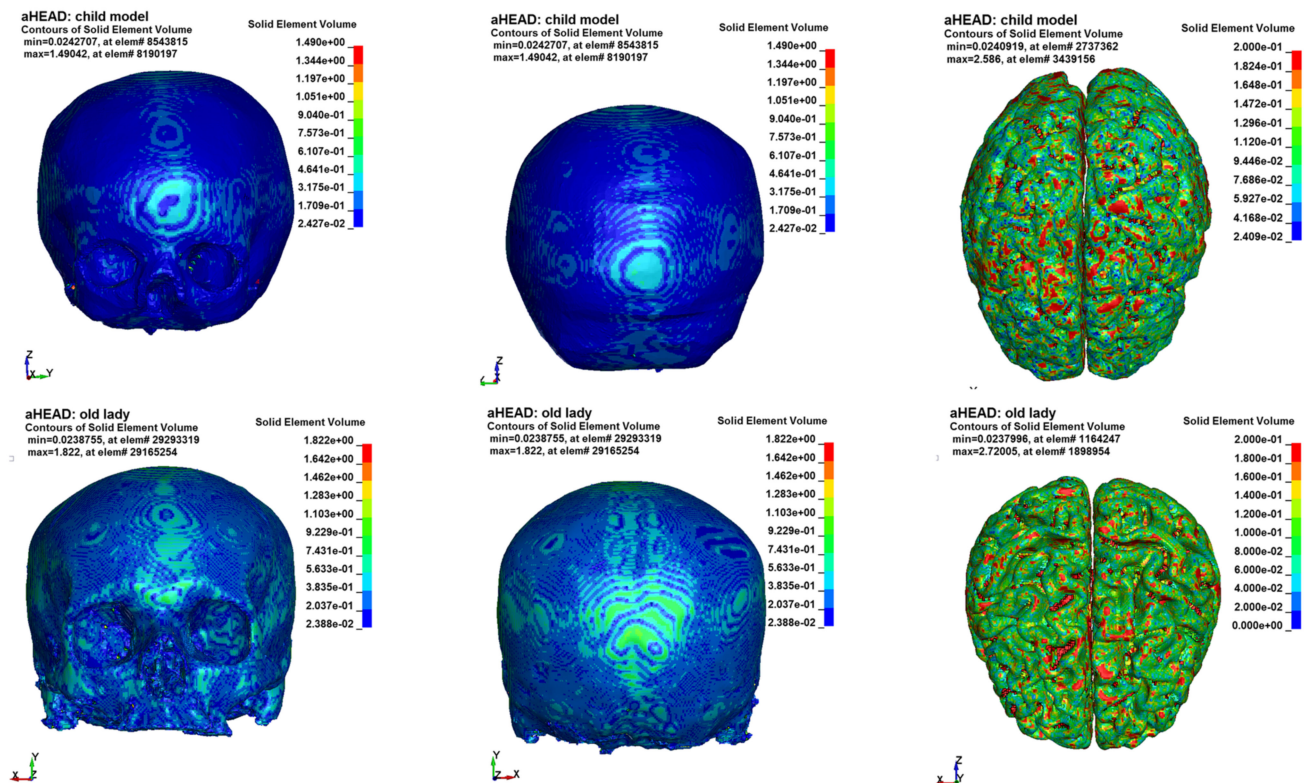
Figure 5. The comparison of head structures and the finite element volume distribution for solid elements in [mm^3]—upper row: 2-year-old and; lower row: 77-year-old head model.
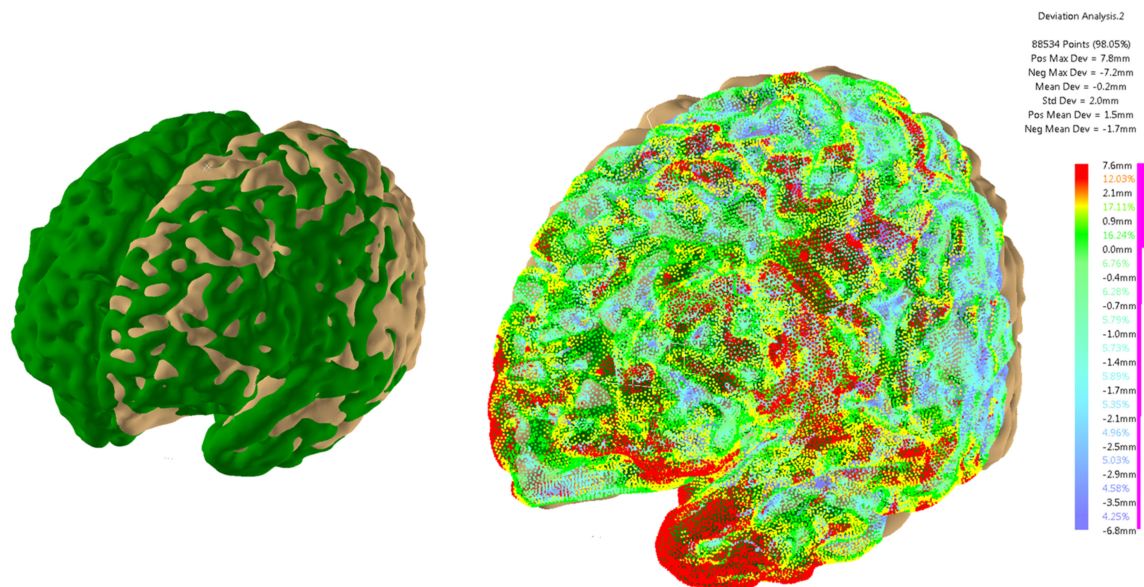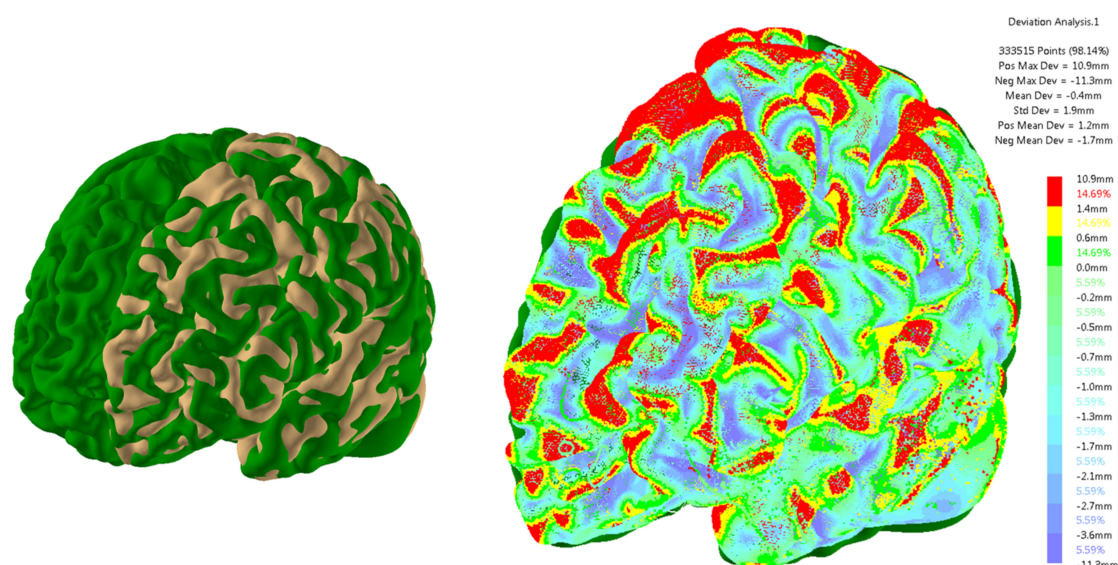

Figure 6. *Cont.*

Figure 6. The deviation analysis of the hemispheres: left: the overlapping mirrored right hemisphere; right: the quantitate comparison analysis in (mm). The result distribution graph is also visible next to the scale. Upper row: 2-year-old and; lower row: 77-year-old brain geometrical surface model.

4. Discussion

Most of the models in the literature are symmetrical and therefore may not fully reflect the biomechanics of the behaviour of brain tissues. This is an issue considering the brain's non-symmetry, clearly observed at its surface level, regarding gyri and sulci structures, which plays an essential role in the local tissue deformations [47,50,61–64]. The folding structure of the brain surface and the non-uniform distribution of the CSF greatly influence the distribution and the magnitude of the maximum stress and strains in the brain [62,63]. Hence, the mapping of the entire geometry of the skull and brain is essential due to the significant differences that affect the results of numerical analyses and the possibility of misinterpretation of the tissue deformation under mechanical load results. It should also be noted that the most popular validation tests of current numerical models are performed on one cerebral hemisphere. Again, it should be emphasised that model validation is necessary for further developing numerical models to ensure that the calculated results correspond to the experimental data. At this point, it is also worth mentioning the current methodology of research on highly deformable tissues. Modern considerations related to biological tissue is based on legacy achievements of metal era material mechanics. Assumptions related to finite displacement, constant volume, and structure homogeneity are inadequate for many natural materials, especially for highly hydrated tissue. The approach taken for the determination of mechanical property should be reconsidered. Modelled as hyper-elastic materials, brain tissue does not meet the basic assumptions mentioned before, leading to a wide discrepancy in mechanical properties given by various researchers.

It should be noted that some differences in physical properties might be explained by age, gender, neurodegenerative diseases, and the region of the taken specimen. Those factors are a source of natural differences. However, factors such as time to test or dehydration level belong to the experimental procedure. It is crucial to decrease the significance of those factors. On the other hand, brain-tissue tests are conducted on a standard tensile machine or as an in-direct method incorporating whole brain-skull-skin structure [58].

The authors want to underline the consequence of assumptions taken for brain tissue. The most significant of a priori taken assumption is symmetry between tension and compression stress state. For most of the engineering materials, this symmetry is in the elastic range even for fatigue loads. Brain tissue does not have proven symmetry for load direction, including normal and shear stresses. Inhomogeneity of brain tissue suggests the anisotropy

of the material. MRI Tractography indicates that the direction of neuron distribution is not evenly distributed. Thus, the axis of anisotropy might be characteristic for each patient. Therefore, extracting samples for the tests has often been randomly oriented, which causes the missing of considered material anisotropy.

By analysing hyper-elastic material formulation, i.e., for Abaqus software [65], it is noticeable that the energy strain potential, U(ε), is a sum of volumetric and deviatoric parts. This means that volumetric energy strain potential is equal as absolute value for the positive and negative hydrostatic stress tensor.

5. Conclusions

In this work, the authors researched the symmetry of the human head. By reviewing the current literature in the field of numerical modelling of adult heads, we concluded that the vast majority of models on the publication market are symmetrical. In the case of the small-child-modelled heads, only one model [50] is not symmetrical—aHEAD 2yo. However, in this work, the authors' numerical models were created without a symmetrical reflection of one side of the head. In the process of segmentation, the entire geometry of the brain and skull were mapped. Special attention was paid to gyri and sulci in the right and left hemispheres of the brain. Research conducted in this work has shown that the head is asymmetrical for the head of an older person and the head of a small child. Both cerebral hemispheres showed the most significant asymmetry in relation to each other. The distribution of geometric deviation is different between the head of a young child and an older person. Greater surface asymmetry can be observed in a small child. As brain tissue degenerates, the brain becomes more symmetrical. These conclusions are supported by medical research in literature [23].

In summary, the current literature needs to be supplemented with more experimental tests of brain tissues and more precise development of numerical models taking into account the entire geometry of the brain as well as data on the age and neurological state of the patient's health. Furthermore, inhomogeneity, internally stored water, and random distribution of neuron fibres are serious factors that might be considered in future research for proper brain mechanics determination. This approach will allow us to gain good insight into the biomechanical response of brain tissues.

References

1.　Evans, C.S.; Wenderoth, P.; Cheng, K. Detection of bilateral symmetry in complex biological images. *Perception* **2000**, *29*, 31–42. [CrossRef]
2.　Kayaert, G.; Wagemans, J. Delayed shape matching benefits from simplicity and symmetry. *Vision Res.* **2009**, *49*, 708–717. [CrossRef]
3.　Sasaki, Y.; Vanduffel, W.; Knutsen, T.; Tyler, C.; Tootell, R. Symmetry activates extrastriate visual cortex in human and nonhuman primates. *Proc. Natl. Acad. Sci. USA* **2005**, *102*, 3159–3163. [CrossRef]
4.　Makin, A.D.J.; Wilton, M.M.; Pecchinenda, A.; Bertamini, M. Symmetry perception and affective responses: A combined EEG/EMG study. *Neuropsychologia* **2012**, *50*, 3250–3261. [CrossRef]
5.　Thornhill, R.; Møller, A.P. Developmental stability, disease and medicine. *Biol. Rev. Camb. Philos. Soc.* **1997**, *72*, 497–548. [CrossRef]

6.   Perrett, D.I.; Burt, D.M.; Penton-Voak, I.S.; Lee, K.J.; Rowland, D.A.; Edwards, R. Symmetry and Human Facial Attractiveness. *Evol. Hum. Behav.* **1999**, *20*, 295–307. [CrossRef]

7.   Wade, T.J. The Relationships between Symmetry and Attractiveness and Mating Relevant Decisions and Behavior: A review. *Symmetry* **2010**, *2*, 1081–1098. [CrossRef]

8.   Gawlikowska, A.; Szczurowski, J.; Czerwiński, F.; Miklaszewska, D.; Adamiec, E.; Dzieciołowska, E. The fluctuating asymmetry of mediaeval and modern human skulls. *HOMO- J. Comp. Hum. Biol.* **2007**, *58*, 159–172. [CrossRef] [PubMed]

9.   Chovalopoulou, M.E.; Papageorgopoulou, C.; Bertsatos, A. Cranium asymmetry in a modern Greek population sample of known age and sex. *Int. J. Legal Med.* **2017**, *131*, 803–812. [CrossRef] [PubMed]

10. Myslobodsky, M.S.; Ingraham, L.J.; Weinberger, D.R. Skull asymmetry and handedness in adults: A possibility of their association with lateral head turning in infancy. *Percept. Mot. Skills* **1987**, *65*, 415–421. [CrossRef]

11. Zilles, K.; Dabringhaus, A.; Geyer, S.; Amunts, K.; Qü, M.; Schleicher, A.; Gilissen, E.; Schlaug, G.; Steinmetz, H. Structural Asymmetries in the Human Forebrain and the Forebrain of Non-Human Primates and Rats. *Neurosci. Biobehav. Rev.* **1996**, *20*, 593–605. [CrossRef]

12. Radosevic, D.; Maric, D.; Ivanovic, D. Human skull base asymmetry analysis. *Int. J. Morphol.* **2020**, *38*, 1566–1570. [CrossRef]

13. Distriquin, Y.; Vital, J.M.; Ella, B. Biomechanical analysis of skull trauma and opportunity in neuroradiology interpretation to explain the post-concussion syndrome: Literature review and case studies presentation. *Eur. Radiol. Exp.* **2020**, *4*, 1–9. [CrossRef]

14. Kong, X.-Z.; Mathias, S.R.; Guadalupe, T.; Working Group, L.; Glahn, D.C.; Franke, B.; Crivello, F.; Tzourio-Mazoyer, N.; Fisher, S.E.; Thompson, P.M.; et al. Mapping cortical brain asymmetry in 17,141 healthy individuals worldwide via the ENIGMA Consortium. *Proc. Natl. Acad. Sci. USA* **2018**, *115*, E5154–E5163. [CrossRef]

15. Duboc, V.; Dufourcq, P.; Blader, P.; Roussigné, M. Asymmetry of the Brain: Development and Implications. *Annu. Rev. Genet.* **2015**, *49*, 647–672. [CrossRef] [PubMed]

16. Geschwind, N.; Levitsky, W. Human brain: Left-right asymmetries in temporal speech region. *Science* **1968**, *161*, 186–187. [CrossRef]

17. Seidenwurm, D.; Roger Bird, C.; Enzmann, D.R.; Marshall, W.H. Left-Right Temporal Region Asymmetry in Infants and Children. *Am. J. Neuroradiol.* **1985**, *6*(5), 777–779. [PubMed]

18. Chi, J.G.; Dooling, E.C.; Gilles, F.H. Gyral development of the human brain. *Ann. Neurol.* **1977**, *1*, 86–93. [CrossRef]

19. Luders, E.; Narr, K.L.; Thompson, P.M.; Rex, D.E.; Jancke, L.; Toga, A.W. Hemispheric asymmetries in cortical thickness. *Cereb. Cortex* **2006**, *16*, 1232–1238. [CrossRef]

20. Schlaug, G.; Jäncke, L.; Huang, Y.; Steinmetz, H. In vivo evidence of structural brain asymmetry in musicians. *Science* **1995**, *267*, 699–701. [CrossRef]

21. Li, S.; Han, Y.; Wang, D.; Yang, H.; Fan, Y.; Lv, Y.; Tang, H.; Gong, Q.; Zang, Y.; He, Y. Mapping surface variability of the central sulcus in musicians. *Cereb. Cortex* **2010**, *20*, 25–33. [CrossRef]

22. Maguire, E.A.; Woollett, K.; Spiers, H.J. London taxi drivers and bus drivers: A structural MRI and neuropsychological analysis. *Hippocampus* **2006**, *16*, 1091–1101. [CrossRef]

23. Roe, J.M.; Vidal-Piñeiro, D.; Sørensen, Ø.; Brandmaier, A.M.; Düzel, S.; Gonzalez, H.A.; Kievit, R.A.; Knights, E.; Kuhn, S.; Lindenberger, U.; et al. Asymmetric thinning of the cerebral cortex across the adult lifespan is accelerated in Alzheimer's Disease. *bioRxiv* **2020**, 1–20. [CrossRef]

24. Mackiewicz, A.; Banach, M.; Denisiewicz, A.; Bedzinski, R. Comparative studies of cervical spine anterior stabilization systems -Finite element analysis. *Clin. Biomech.* **2016**, *32*, 72–79. [CrossRef] [PubMed]

25. Pałka, Ł.; Kuryło, P.; Klekiel, T.; Pruszyński, P. A mechanical study of novel additive manufactured modular mandible fracture fixation plates-Preliminary Study with finite element analysis. *Injury* **2020**, *51*, 1527–1535. [CrossRef]

26. Klekiel, T.; Będziński, R. Finite element analysis of large deformation of articular cartilage in upper ankle joint of occupant in military vehicles during explosion. *Arch. Metall. Mater.* **2015**, *60*, 2115–2121. [CrossRef]

27. Mackiewicz, A.; Sławiński, G.; Niezgoda, T.; Będziński, R. Numerical analysis of the risk of neck injuries caused by IED explosion under the vehicle in military environments. *Acta Mech. Autom.* **2016**, *10*, 258–264. [CrossRef]

28. Bukala, J.; Kwiatkowski, P.; Malachowski, J. Numerical analysis of stent expansion process in coronary artery stenosis with the use of non-compliant balloon. *Biocybern. Biomed. Eng.* **2016**, *36*, 145–156. [CrossRef]

29. Sybilski, K.; Małachowski, J. Impact of Disabled Driver's Mass Center Location on Biomechanical Parameters during Crash. *Appl. Sci.* **2021**, *11*, 1427. [CrossRef]

30. Klekiel, T.; Mackiewicz, A.; Kaczmarek-Pawelska, A.; Skonieczna, J.; Kurowiak, J.; Piasecki, T.; Noszczyk-Nowak, A.; Będziński, R. Novel design of sodium alginate based absorbable stent for the use in urethral stricture disease. *J. Mater. Res. Technol.* **2020**, *9*, 9004–9015. [CrossRef]

31. Arkusz, K.; Klekiel, T.; Sławiński, G.; Będziński, R. Influence of energy absorbers on Malgaigne fracture mechanism in lumbar-pelvic system under vertical impact load. *Comput. Methods Biomech. Biomed. Eng.* **2019**, *22*, 313–323. [CrossRef] [PubMed]

32. Arkusz, K.; Klekiel, T.; Niezgoda, T.M.; Będziński, R. The influence of osteoporotic bone structures of the pelvic-hip complex on stress distribution under impact load. *Acta Bioeng. Biomech. Orig. Pap.* **2018**, *20*. [CrossRef]

33. Ghajari, M.; Hellyer, P.J.; Sharp, D.J. Computational modelling of traumatic brain injury predicts the location of chronic traumatic encephalopathy pathology. *Brain* **2017**, *140*, 333–343. [CrossRef]

34. Zhang, L.; Yang, K.H.; Dwarampudi, R.; Omori, K.; Li, T.; Chang, K.; Hardy, W.N.; Khalil, T.B.; King, A.I. Recent advances in brain injury research: A new human head model development and validation. *Stapp Car Crash J.* **2001**, *45*, 369–394.

35. Zhang, L.; Bae, J.; Hardy, W.N.; Monson, K.L.; Manley, G.T.; Goldsmith, W.; Yang, K.H.; King, A.I. Computational study of the contribution of the vasculature on the dynamic response of the brain. *Stapp Car Crash J.* **2002**, *46*, 145–164. [PubMed]

36. Yang, K.H.; Mao, H.; Wagner, C.; Zhu, F.; Chou, C.C.; King, A.I. *Modeling of the Brain for Injury Prevention*; Springer: Berlin/Heidelberg, Germany, 2011; pp. 69–120.

37. Kleiven, S.; Hardy, W.N. Correlation of an FE Model of the Human Head with Local Brain Motion—Consequences for Injury Prediction. *Stapp Car Crash J.* **2002**, *46*, 123–144.

38. Kleiven, S. Predictors for traumatic brain injuries evaluated through accident reconstructions. *Stapp Car Crash J.* **2007**, *51*, 81–114.

39. Horgan, T.J.; Gilchrist, M.D. The creation of three-dimensional finite element models for simulating head impact biomechanics. *Int. J. Crashworthiness* **2003**, *8*, 353–366. [CrossRef]

40. Takhounts, E.G.; Ridella, S.A.; Hasija, V.; Tannous, R.E.; Campbell, J.Q.; Malone, D.; Danelson, K.; Stitzel, J.; Rowson, S.; Duma, S. Investigation of traumatic brain injuries using the next generation of simulated injury monitor (SIMon) finite element head model. *Stapp Car Crash J.* **2008**, *52*, 1–31.

41. Zong, Z.; Lee, H.P.; Lu, C. A three-dimensional human head finite element model and power flow in a human head subject to impact loading. *J. Biomech.* **2006**, *39*, 284–292. [CrossRef] [PubMed]

42. Belingardi, G.; Chiandussi, G.; Gaviglio, I. Development and Validation of a New Finite Element Model of Human Head. In Proceedings of the 19th International Technical Conference of the Enhanced Safety of Vehicle (ESV), Washington, DC, USA, 6–9 June 2005.

43. Li, X.; Zhou, Z.; Kleiven, S. An anatomically detailed and personalizable head injury model: Significance of brain and white matter tract morphological variability on strain. *Biomech. Model. Mechanobiol.* **2021**, *20*, 403–431. [CrossRef] [PubMed]

44. Mao, H.; Zhang, L.; Jiang, B.; Genthikatti, V.V.; Jin, X.; Zhu, F.; Makwana, R.; Gill, A.; Jandir, G.; Singh, A.; et al. Development of a Finite Element Human Head Model Partially Validated With Thirty Five Experimental Cases. *J. Biomech. Eng.* **2013**, *135*. [CrossRef]

45. Sahoo, D.; Deck, C.; Willinger, R. Development and validation of an advanced anisotropic visco-hyperelastic human brain FE model. *J. Mech. Behav. Biomed. Mater.* **2014**, *33*, 24–42. [CrossRef] [PubMed]

46. Atsumi, N.; Nakahira, Y.; Iwamoto, M. Development and validation of a head/brain FE model and investigation of influential factor on the brain response during head impact. *Int. J. Veh. Saf.* **2016**, *9*, 1. [CrossRef]

47. Fernandes, F.A.O.; Tchepel, D.; Alves de Sousa, R.J.; Ptak, M. Development and validation of a new finite element human head model: Yet another head model (YEAHM). *Eng. Comput.* **2018**, *35*, 477–496. [CrossRef]

48. Ratajczak, M.; Ptak, M.; Chybowski, L.; Gawdzińska, K.; Będziński, R. Material and Structural Modeling Aspects of Brain Tissue Deformation under Dynamic Loads. *Materials* **2019**, *12*, 271. [CrossRef]

49. Zhao, W.; Ruan, S.; Li, H.; Cui, S.; He, L.; Li, J. Development and validation of a 5th percentile human head finite element model based on the Chinese population. *Int. J. Veh. Saf.* **2012**, *6*, 91. [CrossRef]

50. Wilhelm, J.; Ptak, M.; Fernandes, F.A.O.; Kubicki, K.; Kwiatkowski, A.; Ratajczak, M.; Sawicki, M.; Szarek, D. Injury Biomechanics of a Child's Head: Problems, Challenges and Possibilities with a New aHEAD Finite Element Model. *Appl. Sci.* **2020**, *10*, 4467. [CrossRef]

51. Klinich, K.D.; Hulbert, G.M.; Schneider, L.W. Estimating Infant Head Injury Criteria and Impact Response Using Crash Reconstruction and Finite Element Modeling. *Stapp Car Crash J.* **2002**, *46*, 165–194.

52. Roth, S.; Raul, J.-S.; Willinger, R. Biofidelic child head FE model to simulate real world trauma. *Comput. Methods Programs Biomed.* **2008**, *90*, 262–274. [CrossRef]

53. Roth, S.; Vappou, J.; Raul, J.-S.; Willinger, R. Child head injury criteria investigation through numerical simulation of real world trauma. *Comput. Methods Programs Biomed.* **2009**, *93*, 32–45. [CrossRef]

54. Coats, B.; Margulies, S.S.; Ji, S. Parametric study of head impact in the infant. *Stapp Car Crash J.* **2007**, *51*, 1–15.

55. Hardy, W.N.; Foster, C.D.; Mason, M.J.; Yang, K.H.; King, A.I.; Tashman, S. Investigation of Head Injury Mechanisms Using Neutral Density Technology and High-Speed Biplanar X-ray. *Stapp Car Crash J.* **2001**, *45*, 337–368. [PubMed]

56. Fernandes, F.A.O.; Alves de Sousa, R.J.; Ptak, M. Validation of YEAHM. In *Head Injury Simulation in Road Traffic Accidents*; SpringerBriefs in Applied Sciences and Technology; Springer International Publishing: Cham, Switzerland, 2018; pp. 41–58, ISBN1 978-3-319-89926-8; ISBN2 978-3-319-89925-1; ISSN 2191-530X. [CrossRef]

57. Nahum, A.M.; Smith, R.; Ward, C.C. *Intracranial Pressure Dynamics During Head Impact*; SAE Technical Paper 770922; SAE International: Warrendale, PA, USA, 1977. [CrossRef]

58. Hardy, W.N.; Mason, M.J.; Foster, C.D.; Shah, C.S.; Kopacz, J.M.; Yang, K.H.; King, A.I.; Bishop, J.; Bey, M.; Anderst, W.; et al. A study of the response of the human cadaver head to impact. *Stapp Car Crash J.* **2007**, *51*, 17–80.

59. Fernandes, F.A.O.; Alves de Sousa, R.J.; Ptak, M. *Head Injury Simulation in Road Traffic Accidents*; SpringerBriefs in Applied Sciences and Technology; Springer International Publishing: Berlin/Heidelberg, Germany, 2018.

60. Ptak, M.; Kaczyński, P.; Fernandes, F.; de Sousa, R.A. *Computer Simulations for Head Injuries Verification After Impact*; Springer: Berlin/Heidelberg, Germany, 2017; pp. 431–440.

61. Cloots, R.J.H.; Gervaise, H.M.T.; Van Dommelen, J.A.W.; Geers, M.G.D. Biomechanics of traumatic brain injury: Influences of the morphologic heterogeneities of the cerebral cortex. *Ann. Biomed. Eng.* **2008**, *36*, 1203–1215. [CrossRef] [PubMed]

62. Lauret, C.; Hrapko, M.; van Dommelen, J.A.W.; Peters, G.W.M.; Wismans, J.S.H.M. Optical characterization of acceleration-induced strain fields in inhomogeneous brain slices. *Med. Eng. Phys.* **2009**, *31*, 392–399. [CrossRef]

63. Ho, J.; Kleiven, S. Can sulci protect the brain from traumatic injury? *J. Biomech.* **2009**, *42*, 2074–2080. [CrossRef] [PubMed]

64. Toma, M.; Chan-Akeley, R.; Lipari, C.; Kuo, S.-H. Mechanism of Coup and Contrecoup Injuries Induced by a Knock-Out Punch. *Math. Comput. Appl.* **2020**, *25*, 22. [CrossRef]

65. Abaqus Software Hyperelastic Behavior of Rubberlike Materials. Available online: https://abaqus-docs.mit.edu/2017/English/SIMACAEMATRefMap/simamat-c-hyperelastic.htm (accessed on 27 May 2021).